MIPS Calibration at 24 and 70μm
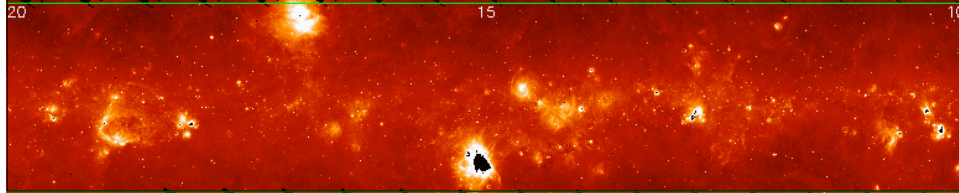
Alberto Noriega-Crespo (MIPS Lead)

on behalf of the Instrument Team (Arizona) &
Instrument Support Team (Spitzer Science Center)

Absolute Calibration and Characterization of the Multiband Imaging Photometer for *Spitzer*. I. The Stellar Calibrator Sample and the 24 μm Calibration

C. W. ENGELBRACHT,[1] M. BLAYLOCK,[1] K. Y. L. SU,[1] J. RHO,[2] G. H. RIEKE,[1] J. MUZEROLLE,[1] D. L. PADGETT,[2] D. C. HINES,[3] K. D. GORDON,[1] D. FADDA,[2] A. NORIEGA-CRESPO,[2] D. M. KELLY,[1] W. B. LATTER,[4] J. L. HINZ,[1] K. A. MISSELT,[1] J. E. MORRISON,[1] J. A. STANSBERRY,[1] D. L. SHUPE,[2] S. STOLOVY,[2] WM. A. WHEATON,[2] E. T. YOUNG,[1] G. NEUGEBAUER,[1] S. WACHTER,[4] P. G. PÉREZ-GONZÁLEZ,[1,5] D. T. FRAYER,[2] AND F. R. MARLEAU[2]

Absolute Calibration and Characterization of the Multiband Imaging Photometer for *Spitzer*. II. 70 μm Imaging

KARL D. GORDON,[1] CHARLES W. ENGELBRACHT,[1] DARIO FADDA,[2] JOHN STANSBERRY,[1] STEFANIE WACHTER,[2] DAVE T. FRAYER,[2] GEORGE RIEKE,[1] ALBERTO NORIEGA-CRESPO,[2] WILLIAM B. LATTER,[4] ERICK YOUNG,[1] GERRY NEUGEBAUER,[1] ZOLTAN BALOG,[1] JEFFREY W. BEEMAN,[4] HERVÉ DOLE,[6] ERICH EGAMI,[1] EUGENE E. HALLER,[4,6] DEAN HINES,[7] DOUG KELLY,[1] FRANCINE MARLEAU,[2] KARL MISSELT,[1] JANE MORRISON,[1] PABLO PÉREZ-GONZÁLEZ,[1,8] JEONGHEE RHO,[2] AND WM. A. WHEATON[2]

Outline

- MIPS Summary
- Zero Points (Rieke Photometric System)
- Repeatability
- Linearity
- Comparison with IRAS
- Extended Source Calibration

MIPS Summary

MULTIBAND IMAGING PHOTOMETER FOR SPITZER (MIPS) http://ssc.spitzer.caltech.edu/mips/
Pocket Guide

Basic MIPS Capabilities:

Imaging photometry at 24, 70, and 160 µm and low resolution (R = 15 – 25) spectroscopy between 52 and 97 µm. A fine pixel scale option at 70 µm (no change required for the other two bands), combined with precise subpixel sampling dither patterns, allow data processing to achieve "super resolution" imaging. A cryogenic scan mirror mechanism provides freeze frame scan mapping, efficient dithering, and other instrument capabilities.

The MIPS Astronomical Observation Templates:

Photometry & Super Resolution
- Telescope staring mode imaging photometry
Scan Mapping
- Freeze frame mapping in all three bands with constant telescope slewing
Spectral Energy Distribution (SED)
- Low resolution (R = 15 – 25) spectroscopy over 52 to 97 µm
Total Power Mode
- Zero level brightness of very extended emission

MIPS Instantaneous Fields of View:

24 µm	5.4×5.4 arcminutes
70 µm	5.25×2.6 or 2.6×1.3 arcminutes
160 µm	0.53×5.33 arcminutes (effective)
SED Slit	2.0×0.33 arcminutes (full wavelength coverage)

The MIPS Detector Arrays:

24 µm	Si:As (IBC)
	128x128 pixels; 2.55"
	4.7 µm bandwidth
70 µm	Ge:Ga
	32x32 pixels; 5.3" or 9.96"
	19 µm bandwidth
	SED R = 15 – 25 (9.8" pixels)
160 µm	Stressed Ge:Ga
	2x20 pixels; 16.0"x18.0"
	35 µm bandwidth

Basic Sensitivities (low background):
5 sigma in 500 seconds on source

24 µm	110 µJy
70 µm default	7.2 mJy
70 µm fine	14.4 mJy
SED	82/201/447 mJy @ 60/75/90 µm
160 µm	29 (40 w/ confusion) mJy

Saturation Limits:
Point source in 1 second (Jy); Extended source in 10 seconds (MJy/ster)

Band	Point Source	Extended
24 µm	4.1	260
70 µm (default)	23	101
70 µm (fine)	57	292
SED @ 60,75,90µm	250/290/1000	1087/1261/4350
160 µm	3	20

Prepared by:
William B. Latter
SSC/MIPS Instrument Support Team Lead

(v7.0, updated 31 October 06, JWC)

24μm Calibration - Summary

- The primary calibrators are A stars (22 sample)

- Calibration factor (from instrumental units to astrophysical units) = 4.54 10^{-2} MJy/sr/DN/s

- Absolute uncertainty = 4%

- After 2.5yrs: 348 measurements of 141 stars (covering a factor 460 in flux density) from 8.6mJy up to 4 Jy

- Repeatability for HD 159330 (routine calibrator) shows a rms scatter of 0.4%

- The calibration is based on the standard 3sec photometric observation (agrees within 1% with Scan mode)

24μm Post-Processing
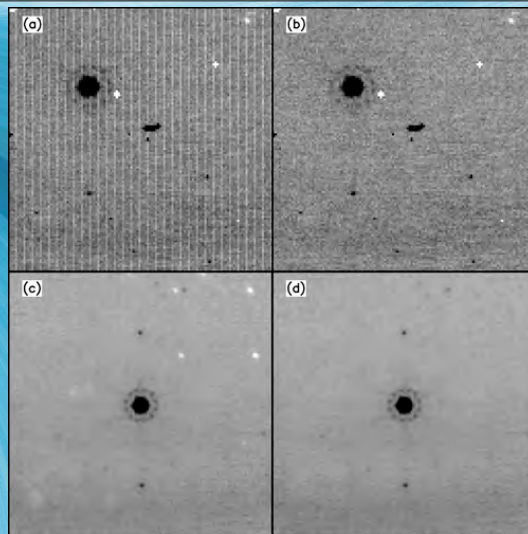
Fig. 1.— Artifacts not discussed by Gordon et al. (2005) that are now fixed as part of standard processing with the MIPS Data Analysis Tool (DAT), illustrated using observations of HD 159330 (AOR key 13587712) plotted in reverse gray scale. (a) The jailbar effect is most easily seen in individual frames, here caused by a cosmic ray below and to the right of the star, and (b) fixed as described in § 2. (c) The spots caused by debris on the pick-off mirror (several sharp white spots above and to the right of the star, as well as diffuse white regions below and to the left of the star) are most easily seen in a mosaicked image and are (d) fixed using separate flat fields for each scan mirror position.

24μm
Artifacts

Fig. 2.— Artifacts not removed by standard processing with the MIPS DAT, plotted in reverse gray scale. As discussed in § 2, (a) gain changes imposed by previous observations (illustrated using a single-frame observation of HD 159330, AOR key 12195328) are (b) removed using a second flat field. (c) Background changes as a function of scan mirror position (illustrated using a mosaic observation of HD 106965, AOR key 13201920) are (d) removed before mosaicking. For the targets discussed here, the effects of (e) residual images (circled; illustrated using a mosaic observation of HD 159330, AOR key 12195328) and (f) sources that saturate in 3 s (illustrated using a single-frame observation of HD 180711, AOR key 9805568) are small and we make no correction.

Galactic center (l= 0.5-2.5, b=+0.5)

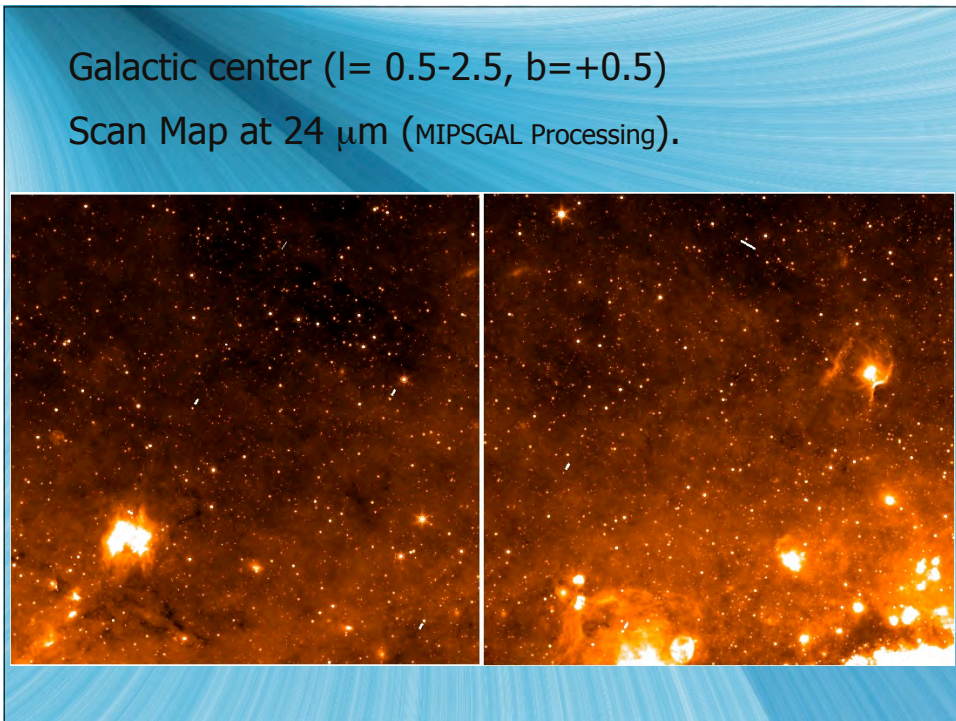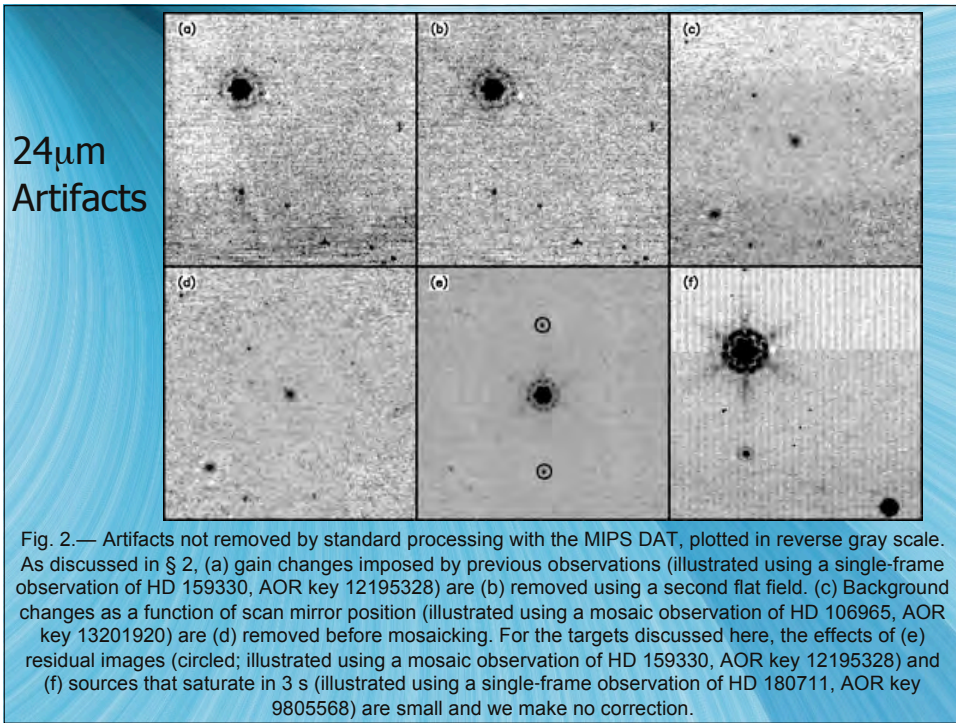Scan Map at 24 μm (MIPSGAL Processing).

TABLE 3
Data Used to Compute the 24 μm Calibration Factor

Name	K_s^a (mag)	24 μm Count Rate (DN s^{-1})	Uncertainty (DN s^{-1})	Calibration Factor (MJy sr^{-1} [DN s^{-1}]$^{-1}$)	Uncertainty (MJy sr^{-1} [DN s^{-1}]$^{-1}$)
HD 000319	5.479	6.708E+03	5.00E+01	4.513E−02	1.39E−03
HD 002811	7.057	1.591E+03	3.35E+01	4.448E−02	1.63E−03
HD 011413	5.422	7.866E+03	3.87E+01	4.056E−02	1.23E−03
HD 014943	5.439	7.180E+03	2.84E+01	4.374E−02	1.32E−03
HD 015646	6.411	2.997E+03	4.85E+01	4.281E−02	1.46E−03
HD 017254	5.877	4.529E+03	1.97E+01	4.632E−02	1.40E−03
HD 020888	5.691	5.519E+03	2.04E+01	4.512E−02	1.36E−03
HD 021981	5.526	6.089E+03	1.33E+01	4.761E−02	1.43E−03
HD 034868	6.024	3.851E+03	3.89E+01	4.758E−02	1.51E−03
HD 042525	5.751	5.116E+03	2.85E+01	4.606E−02	1.40E−03
HD 057336	7.114	1.403E+03	3.44E+01	4.786E−02	1.86E−03
HD 073210	6.165	3.707E+03	5.55E+01	4.341E−02	1.45E−03
HD 073666	6.532	2.541E+03	5.66E+01	4.517E−02	1.69E−03
HD 073819	6.280	3.170E+03	5.29E+01	4.566E−02	1.57E−03
HD 092845	5.513	7.166E+03	4.51E+01	4.094E−02	1.26E−03
HD 101452	6.819	1.910E+03	3.50E+01	4.613E−02	1.62E−03
HD 105805	5.600	5.734E+03	5.10E+01	4.722E−02	1.48E−03
HD 116706	5.502	6.188E+03	5.01E+01	4.789E−02	1.49E−03
HD 128998	5.756	4.824E+03	2.79E+01	4.862E−02	1.48E−03
HD 158485	6.145	3.564E+03	2.79E+01	4.599E−02	1.43E−03
HD 163466	6.339	2.917E+03	2.94E+01	4.699E−02	1.49E−03
HD 172728	5.753	4.747E+03	2.21E+01	4.954E−02	1.50E−03

Note.—The average calibration factor is 4.54 × 10^{-2} MJy sr^{-1} (DN s^{-1})$^{-1}$, to which we have assigned an uncertainty of 2% (see § 3).
^{a} K_s = [24] for the stars in this table (see G. H. Rieke et al. 2007, in preparation), all of which are between types A0 and A6.

The zero point is derived from a set of well measured

A type stars (22)

Repeatability is 0.4% over the first 1000 days.
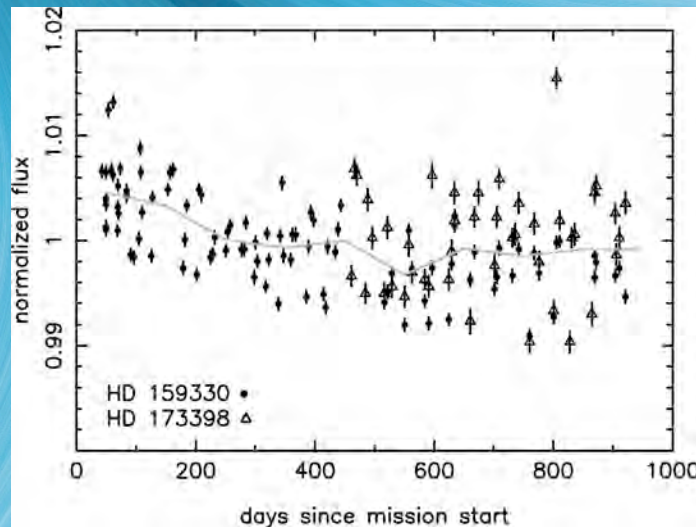
Departure from linearity is 0.3% between 9 and 4000 mJy
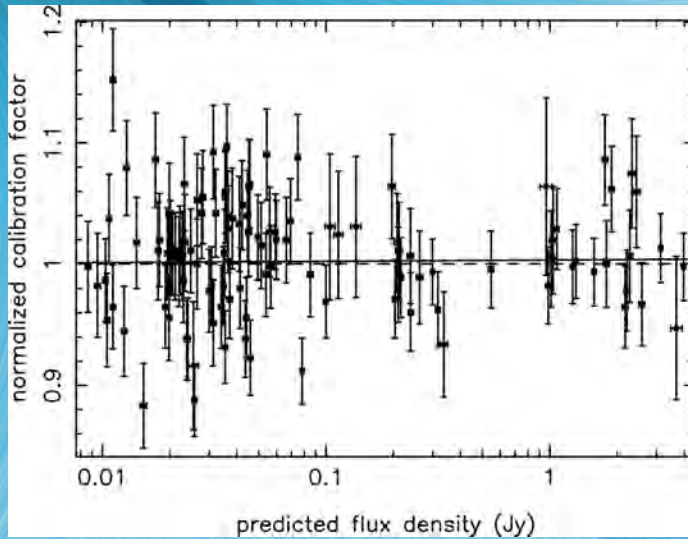
IRAS 12 & 25μm and MIPS 24μm

[point sources]

Measured:

$F(24\mu m)/F(12\mu m) = 0.265$

$F(24\mu m)/F(25\mu m) = 1.11$

Predicted (Kurucz's Models):

$F(24\mu m)/F(12\mu m) = 0.266$

$F(24\mu m)/F(25\mu m) = 1.11$
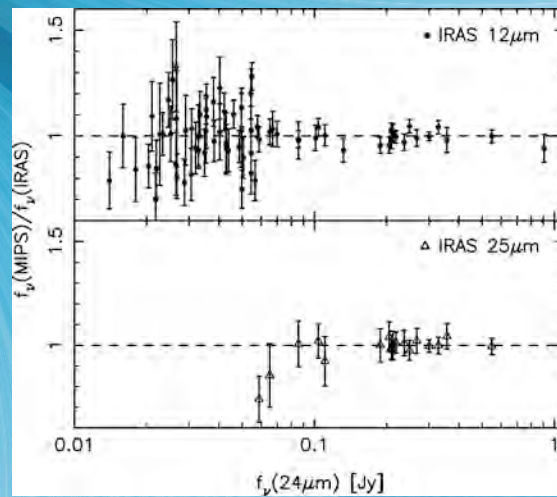
No obvious effects due to background, but the measurement is noisy.
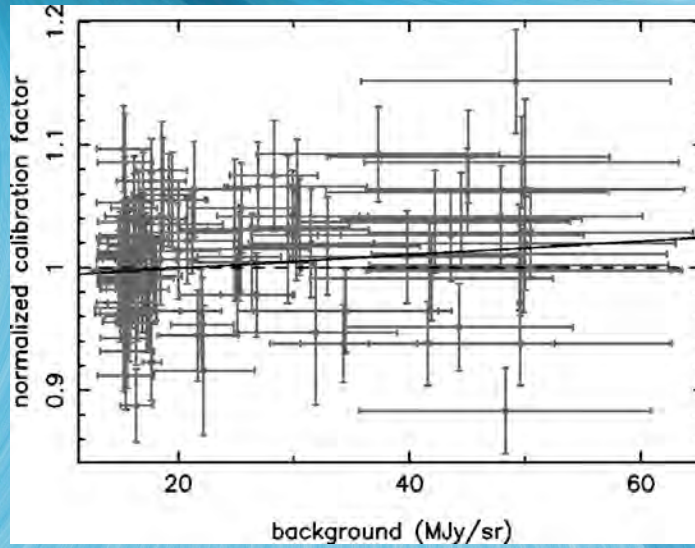
24μm Extended Source Calibration
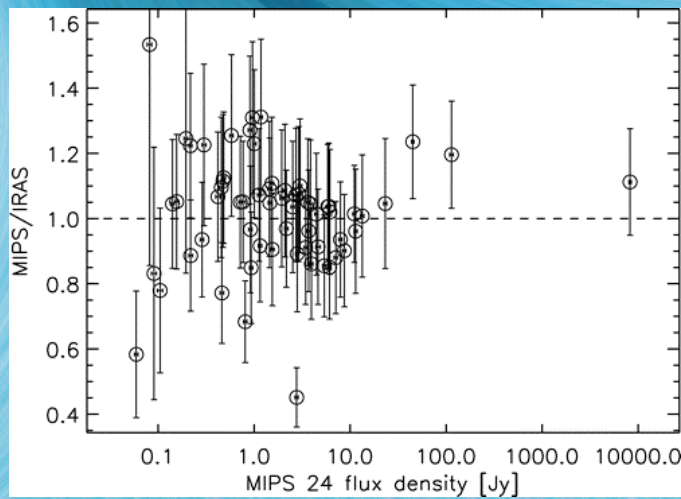
75 SINGS galaxies plus M31 & LMC

MIPS/IRAS = 0.96 (within 8% instrumental uncertainties)

Fig. 10.— Ratio of MIPS to IRAS measurements of extended sources as a function of flux density measured at 24 μm. The error bars represent the combined uncertainty on both measurements. The dashed line is drawn at 1 as a guide.

70um Calibration - Summary

• The predicted colors at 70μm are derived from those 24μm (ratio of the 23.675 and 71.42μm effective wavelengths with the appropriate Kurucz model).

• The Wide Field (WF) calibration factor is 702 +/- 35 Mjy/sr/MIPS70 based on 66 stars.

• Absolute uncertainty = 7%

• The WF calibration covers a flux density range 22mJy to 17Jy

• The zero point at 71.42μm (Rieke Photometric System) is 0.778+/- 0.012

• The photometric repeatability is 4.5%

• The calibration is based on the standard WF photometry observations (3 and 10sec)

70μm Post-Processing
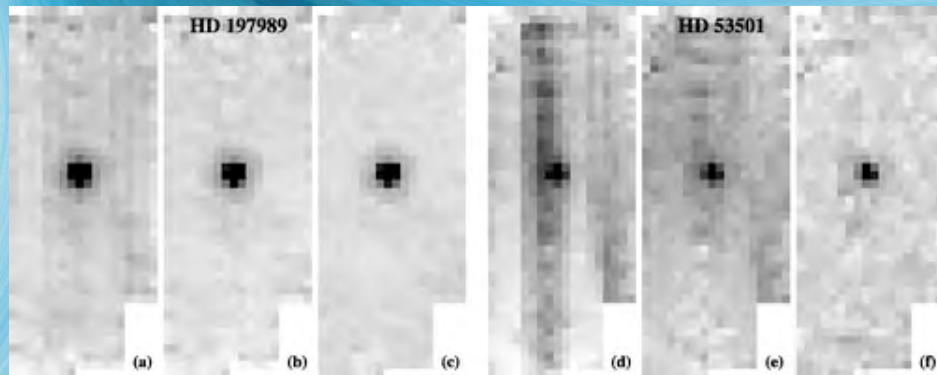
Fig. 1.— Mosaics of coarse-scale observations of two stars of different brightness shown with (a, d) default reductions, (b, e) column mean subtraction, and (c, f) column mean subtraction and time filtering. The two stars are HD 197989 (AOR key 13590784, $\mathrm{flux}\,\,\mathrm{density}\,=787$ mJy) and HD 53501 (AOR key 13641984, $\mathrm{flux}\,\,\mathrm{density}\,=135$ mJy). The HD 197989 images are displayed with a linear stretch that ranges (a) from 0.022 to 0.05, (b) from −0.005 to 0.025, and (c) from −0.005 to 0.0025. The HD 53501 images are displayed with a linear stretch that ranges (d) from 0.009 to 0.025, (e) from −0.005 to 0.01, and (f) from −0.002 to 0.008. The images and ranges are all given in MIPS70 units.

Fig. 1.— The M31 MIPS images. The images are scaled using a quadratic root (x0.25) between −0.1 and 3 MJy sr−1 (24 μm), 0.1 and 35 MJy sr−1 (70 μm), and 0 and 90 MJy sr−1 (160 μm). The bottom image is a three-color composite of the MIPS images (with scaling adjusted to emphasize the differences between bands); the color gives an indication of the dust temperature. The images are oriented with a nominal position angle of M31 (38°) horizontal and are cropped to a common size. The nearly vertical streaks present in the 70 and 160 μm images are residual Ga:Ge detector instrumental signatures. M32 is clearly detected at 24 μm, but not in the other two MIPS bands. NGC 205 is detected in all three MIPS bands but is located northwest of M31 beyond the

Linearity Check
Cal. Factor = 702 +/-35 Mjy/sr/MIPS70 (5%)

From 22mJy to 17Jy

66 stars
1st 2.5 yrs

Based on PSF photometry (aper. Phot =704 0.3-1Jy

Fig. 4.— Average calibration factor for each star vs. predicted flux density (a, b) and background (c, d). The dashed line is drawn at the final calibration factor. The solid line gives the linear fit to all the data except for the five stars with boxes. These stars were rejected from the fit, as they are > $5\,\sigma$ from the mean.

70μm
Repeatability

2.9%
2.7%
4.5%
3.7%

● HD 163588
○ HD 180711

Fig. 6.— Normalized flux densities for the two repeatability stars, HD 163588 and HD 180711, vs. time. The solid line gives the sigma-clipped average in 15 equally spaced bins. The dashed line is drawn at 1. The typical uncertainty of a single measurement is shown in the upper right. The first vertical line indicates the transition between dither patterns (between second and third MIPS campaigns). The second vertical line indicates the transition between array bias voltage values (between fourth and fifth MIPS campaigns). The third vertical line indicates the update to the instrument software (between the eighth and ninth MIPS campaigns).

Extended Emission Photometry Check

Average
MIPS/IRAS =
0.99

75 SINGS
Galaxies plus
M31, M33,
LMC & M101

Fig. 9.— Ratio of MIPS 70 μm measured flux density to the 70 μm flux density predicted from IRAS 60 and 100 μm measurements shown as a check of the extended source calibration. The sample shown is comprised of the 75 SINGS galaxies supplemented by the LMC, M31, M33, and M101. The uncertainties are computed from the uncertainties in the IRAS and MIPS measurements. The dashed line is drawn at a value of 1.